NASA TM X-141

TECHNICAL MEMORANDUM
X-141

STATIC STABILITY CHARACTERISTICS OF THREE THICK WING MODELS WITH PARABOLIC PLAN FORMS AT A MACH NUMBER OF 3.11

By M. J. Queijo

Langley Research Center
Langley Field, Va.

NATIONAL AERONAUTICS AND SPACE ADMINISTRATION
WASHINGTON

October 1959
Declassified September 1, 1961

NATIONAL AERONAUTICS AND SPACE ADMINISTRATION

TECHNICAL MEMORANDUM X-141

STATIC STABILITY CHARACTERISTICS OF THREE THICK WING MODELS WITH PARABOLIC PLAN FORMS AT A MACH NUMBER OF 3.11

By M. J. Queijo

SUMMARY

An experimental investigation has been made to determine the static stability characteristics of three thick wing models with parabolic plan forms at a Mach number of 3.11 for angles of attack from about -6° to 16°. The primary variable was aspect ratio, with the plan-form area and the ratio of base height to span kept the same for all three models.

All models had stable, linear pitching-moment curves about the quarter chord of the wing mean aerodynamic chord. The model with the lowest aspect ratio attained a maximum untrimmed lift-drag ratio of about 5.0 at an angle of attack of about 8°. Increasing the aspect ratio (which was accompanied by an increase in base area because the ratio of the base height to span was kept constant) caused a decrease in maximum lift-drag ratio.

All models were directionally stable for the range of angle of attack of the tests. Addition of a vertical tail to the models caused an increase in the directional stability over the angle-of-attack range. In general, the lateral aerodynamic characteristics of the models were not linear functions of angle of attack over any appreciable angle-of-attack range.

INTRODUCTION

Hypersonic gliders have been of interest because of possible application as military or commercial vehicles. Since such vehicles operate in the atmosphere at very high speeds, they must be designed to withstand severe aerodynamic heating, which generally dictates the use of

blunt noses on bodies and a combination of blunt leading edge and high sweep on wings. (See, e.g., refs. 1, 2, and 3.) As pointed out in reference 2, one is led to consider hypersonic configurations consisting of blunt bodies and highly swept, thick, triangular-plan-form wings. A slight departure from the triangular plan form is the parabolic plan form, which incorporates high sweep with a blunt leading edge. It appears that, at least from heating considerations, a thick parabolic-plan-form wing might be a reasonable hypersonic configuration.

Other considerations of importance in hypersonic-glider design are lift-drag ratios (which are a measure of performance efficiency) and stability characteristics. The purpose of the present investigation was to determine the static longitudinal and lateral aerodynamic characteristics of a series of three thick parabolic-plan-form wings which might be of interest for application to boost-glide vehicles. The major geometric variable in the series was the plan-form aspect ratio.

SYMBOLS

The data presented herein are referred to the stability system of axes shown in figure 1. Moments are given about a moment center located at the projection of the quarter chord of the wing mean aerodynamic chord on the wing plane of symmetry. The symbols and coefficients used are defined as follows:

A	plan-form aspect ratio, b^2/S
b	span, ft
c	chord, ft
$\bar{c}$	mean aerodynamic chord, $\frac{2}{S}\int_0^{b/2} c^2 dy$, ft
q	dynamic pressure, $\frac{1}{2}\rho V^2$, lb/sq ft
S	plan-form area, sq ft
V	free-stream velocity, ft/sec
X,Y,Z	stability axes
x,y,z	model coordinates
α	angle of attack, deg

β sideslip angle, deg

ρ mass density, slugs/cu ft

C_L lift coefficient, Lift/qS

C_D drag coefficient, Drag/qS

C_Y side-force coefficient, Side force/qS

C_m pitching-moment coefficient, Pitching moment/$qS\bar{c}$

C_l rolling-moment coefficient, Rolling moment/qSb

C_n yawing-moment coefficient, Yawing moment/qSb

$C_{Y_\beta} = \partial C_Y / \partial \beta$

$C_{l_\beta} = \partial C_l / \partial \beta$

$C_{n_\beta} = \partial C_n / \partial \beta$

$L/D = C_L / C_D$

MODELS

The geometric characteristics of the wing models used in this investigation are given in figure 2. All models had parabolic plan forms and had the same plan-form area of 0.278 square foot. The aspect ratios were 0.63, 0.86, and 1.24. Cross sections normal to the plane of symmetry were semiellipses with the flat side forming the bottom of the wing. The bases of the models all had the same height-span ratio; hence, the higher the aspect ratio the greater the base area.

The wing models were constructed of fiber glass and Paraplex bonded on steel cores. The steel cores were bored to fit over a six-component electrical strain-gage balance. The triangular vertical tails were made of steel and had blunt wedge airfoil sections. Details of the tails are given in figure 3.

A photograph of one of the models is given in figure 4.

APPARATUS AND TESTS

The tests were made in the Langley gas dynamics laboratory in a jet of the intermittent type having a high-pressure reservoir and exhausting into the atmosphere. The two-dimensional nozzle has a square test section approximately 12 inches by 12 inches and is equipped with a short diffuser. All tests were made at a stagnation pressure of about 74 lb/sq in. gage (about 88.7 lb/sq in. abs.) and a temperature of 100° F. The Reynolds number of the tests was about 12.6×10^6 per foot.

The angle-of-attack range of the tests was from about -6° to 16° and was limited by the load capacities of the strain-gage balance. Sideslip data were obtained at sideslip angles of -3°, 0°, 3°, and 6°. At each angle of attack and sideslip, measurements were made of normal, axial, and side forces and of pitching, rolling, and yawing moments. The measurements were made by means of a sting-supported electrical strain-gage balance which fitted inside the models. The balance and models rotated on an angle-of-attack mechanism which kept the models centered in the tunnel. Sideslip angles were obtained by the use of bent stings.

Base pressure was measured throughout the angle-of-attack range for each model. The measured pressures were used to calculate the axial force acting at the base of the models. The axial forces measured by the strain gages were corrected to the condition of free-stream static pressure acting at the base.

RESULTS AND DISCUSSION

No analysis of the results of this investigation is presented; however, the results of most interest are pointed out in this section.

Longitudinal Characteristics

The longitudinal characteristics C_L, C_D, and C_m of the models with tail off are presented in figure 5 as functions of angle of attack. The lift and pitching-moment curves are approximately linear for the angle-of-attack range of the test. All wings had longitudinal stability about the quarter chord of the wing mean aerodynamic chord. Generally, increasing the wing aspect ratio caused increases in the lift-curve slope and the longitudinal stability. Increasing the wing aspect ratio increased the angle of zero lift because of the curvature of the upper surface of the wings. Increasing the wing aspect ratio from 0.63 to 1.24, with its accompanying increase in wing thickness, caused a large

increase in wing drag. The changes in drag coefficient caused corresponding changes in the lift-drag ratio. The 0.625-aspect-ratio wing had a maximum value of L/D for untrimmed conditions of about 5 at an angle of attack of 8°, whereas the 1.24-aspect-ratio wing had a lift-drag ratio of 1.3 at the same angle of attack. The maximum value of L/D of the 1.24-aspect-ratio wing was not reached in these tests; however, the results indicate that maximum L/D decreases and the angle of attack for maximum L/D increases as the aspect ratio and thickness are increased.

Addition of the vertical tails to the wing models produced no appreciable effects on the longitudinal characteristics. (Compare figs. 5 and 6.)

Lateral Characteristics

The static lateral-stability parameters C_{n_β}, C_{l_β}, and C_{Y_β} for the three wing models are plotted as functions of angle of attack in figure 7(a). All wings had directional stability $\left(\text{positive } C_{n_\beta}\right)$ and negative effective dihedral $\left(\text{positive } C_{l_\beta}\right)$ for the selected moment center throughout the angle-of-attack range of the tests. In general, C_{l_β} became less positive as the angle of attack was increased.

Addition to the wing of a triangular vertical tail with a wedge airfoil section increased the directional stability of the models over the angle-of-attack range. (See figs. 7(a) and 7(b).) In general, the lateral aerodynamic characteristics of the models were not linear functions of angle of attack over any appreciable angle-of-attack range.

CONCLUDING REMARKS

An experimental investigation has been made to determine the static stability characteristics of three thick wing models with parabolic plan forms at a Mach number of 3.11 for angles of attack from about -6° to 16°. The primary variable was aspect ratio, which varied from 0.63 to 1.24. The plan-form area and the base height-span ratio were kept the same for all three models.

All models had stable linear pitching-moment curves about the quarter chord of the wing mean aerodynamic chord. The model having the lowest aspect ratio attained a maximum untrimmed lift-drag ratio of about 5.0 at an angle of attack of about 8°. Increasing the aspect ratio (which was

accompanied by an increase in base area because the base height-span ratio was kept constant) caused a decrease in maximum lift-drag ratio.

All models were directionally stable for the range of angle of attack of the tests. Addition of a vertical tail to the models caused an increase in the directional stability over the angle-of-attack range. In general, the lateral aerodynamic characteristics of the models were not linear functions of angle of attack over any appreciable angle-of-attack range.

Langley Research Center,
National Aeronautics and Space Administration,
Langley Field, Va., July 29, 1959.

REFERENCES

1. Allen, H. Julian, and Eggers, A. J., Jr.: A Study of the Motion and Aerodynamic Heating of Ballistic Missiles Entering the Earth's Atmosphere at High Supersonic Speeds. NACA Rep. 1381, 1958. (Supersedes NACA TN 4047.)

2. Eggers, Alfred J., Jr., Allen, H. Julian, and Neice, Stanford E.: A Comparative Analysis of the Performance of Long-Range Hypervelocity Vehicles. NACA TN 4046, 1957. (Supersedes NACA RM A54L10.)

3. Lange, Roy H.: Exploratory Investigation at a Mach Number of 5.20 of the Longitudinal Aerodynamic Characteristics of Flat-Bottom Bodies. NACA RM L56E30, 1956.

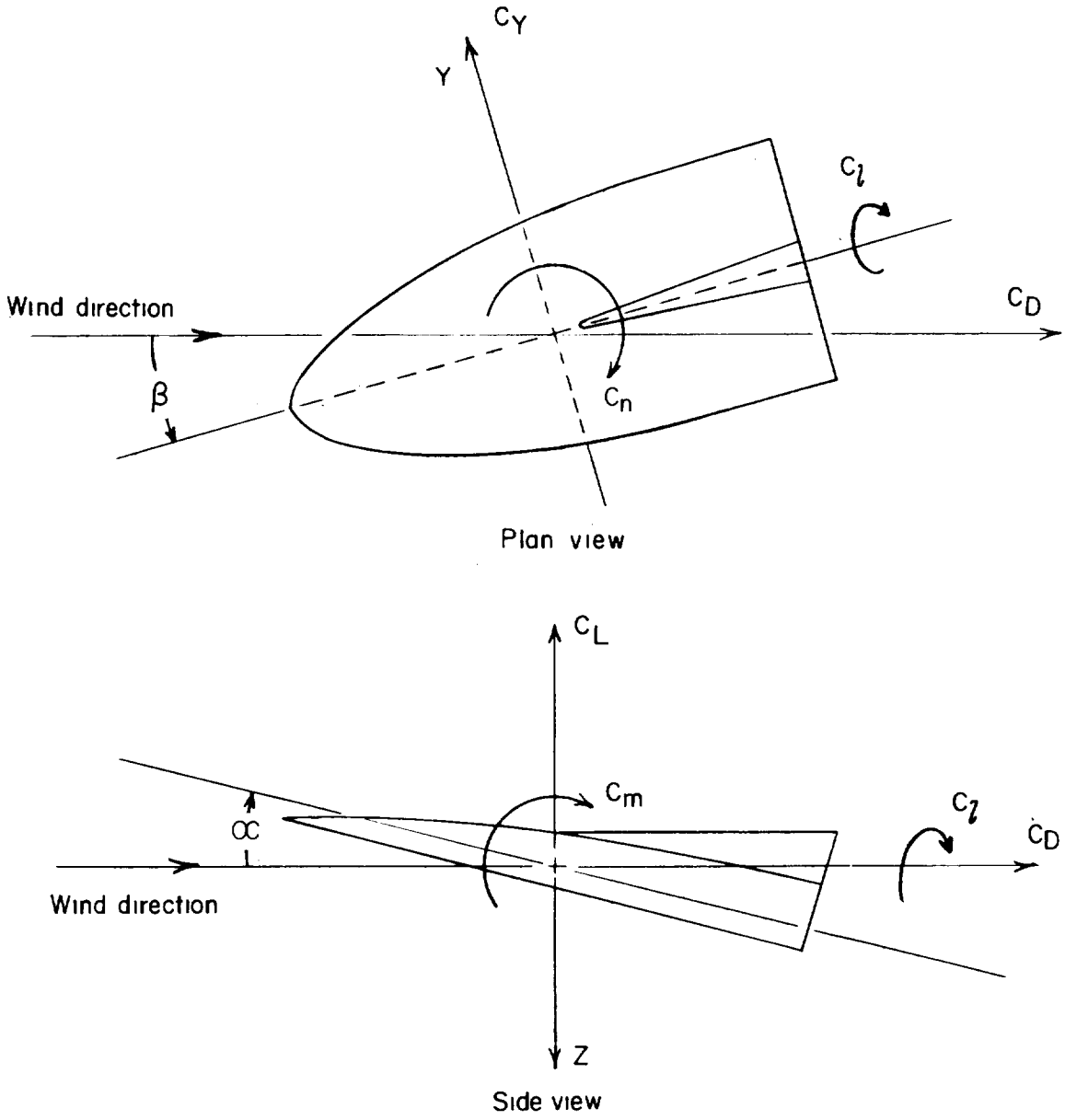

Figure 1.- Stability axes system. Arrows indicate positive directions of displacements, forces, and moments.

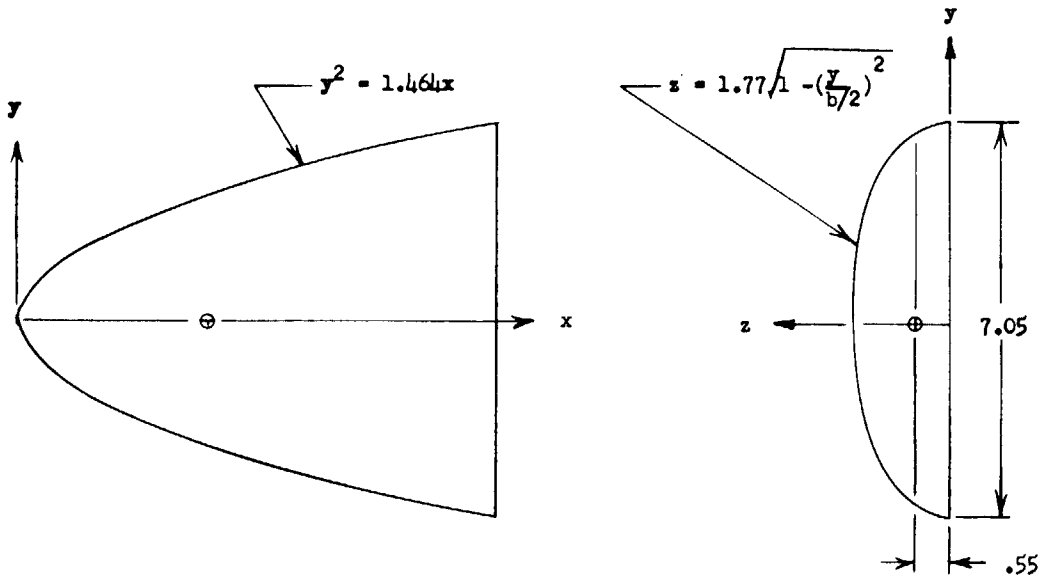

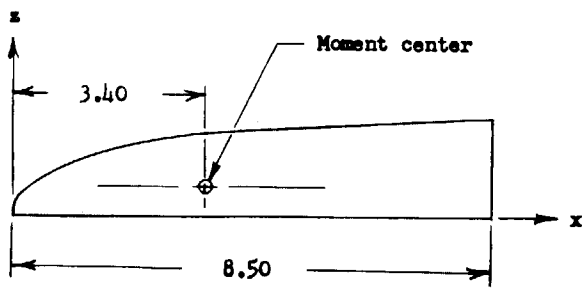

Side-view coordinates

x	z
.20	.45
.40	.58
.60	.70
1.00	.94
2.00	1.26
3.00	1.46
4.25	1.59
8.50	1.77

(a) Aspect ratio 1.24.

Figure 2.- Geometric characteristics of wing models. All dimensions are in inches.

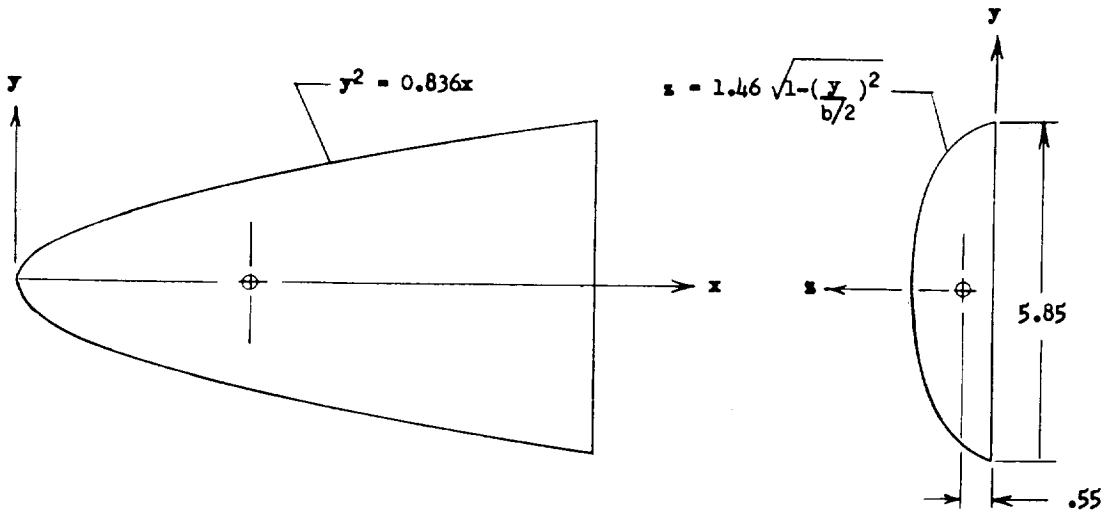

Side-view coordinates

x	z
.25	.30
.50	.41
1.00	.62
1.50	.80
2.50	1.05
4.00	1.25
5.00	1.32
10.25	1.46

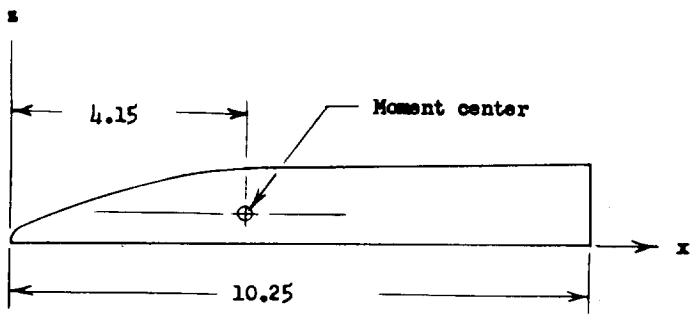

(b) Aspect ratio 0.83.

Figure 2.- Continued.

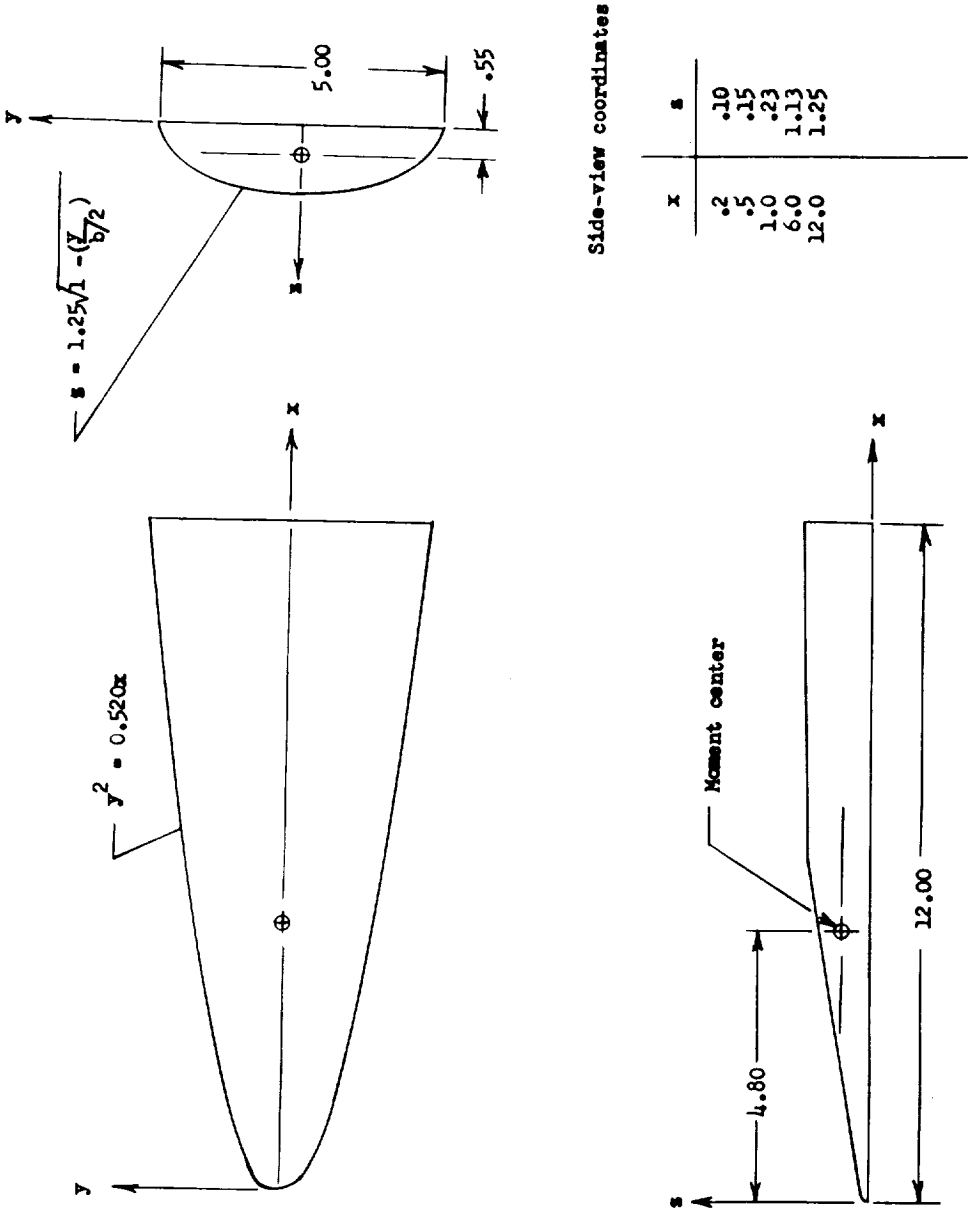

(c) Aspect ratio 0.63.

Figure 2.- Concluded.

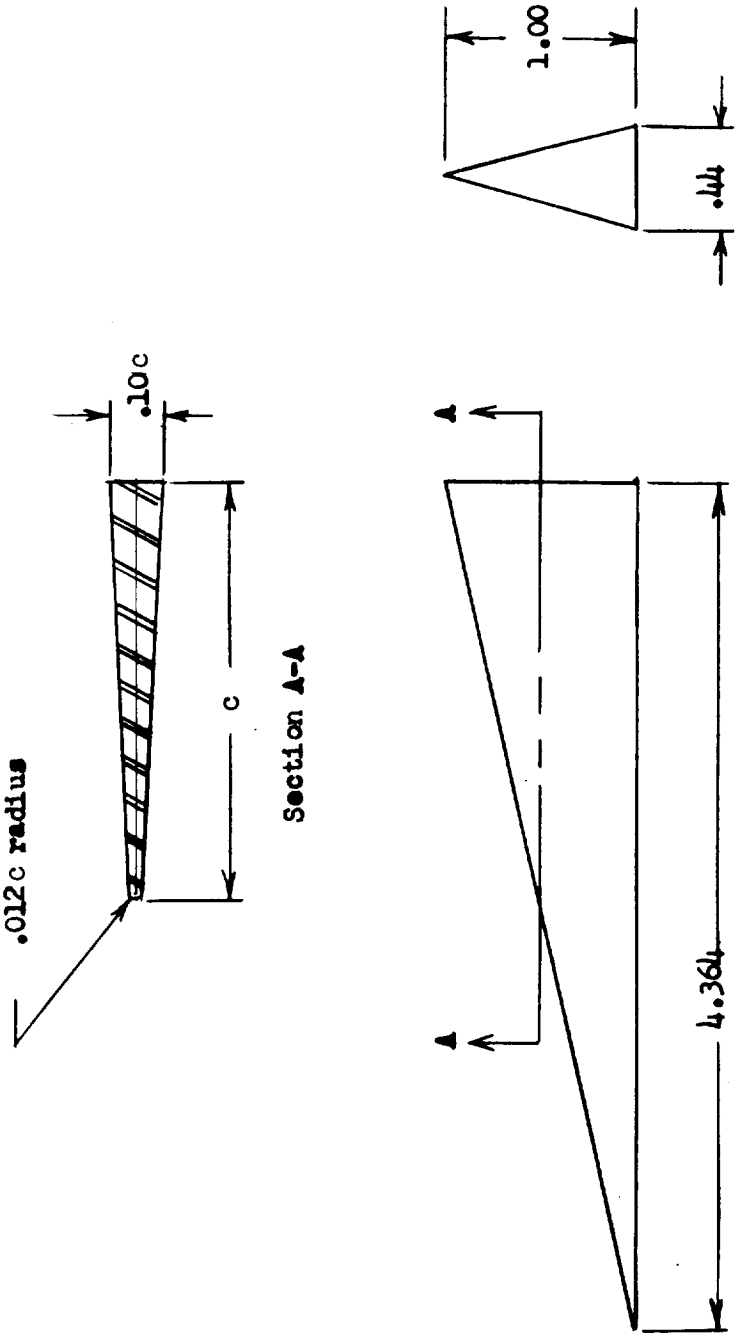

Figure 3.- Vertical tail used on wing models. All dimensions are in inches.

Figure 4.- Photograph of 0.63-aspect-ratio model with vertical tail. L-57-5356

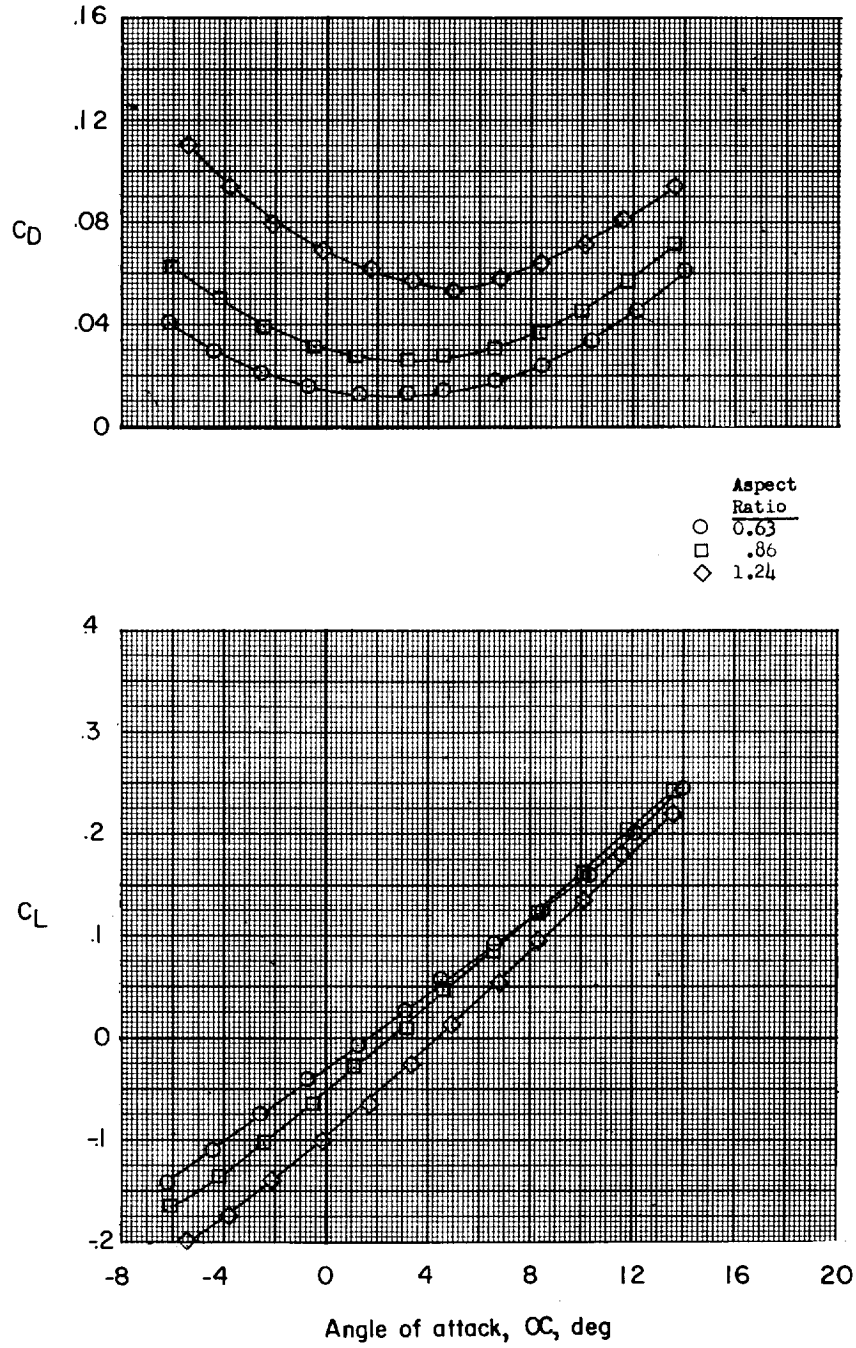

(a) Lift and drag characteristics.

Figure 5.- Longitudinal characteristics of wing models. Vertical tail off.

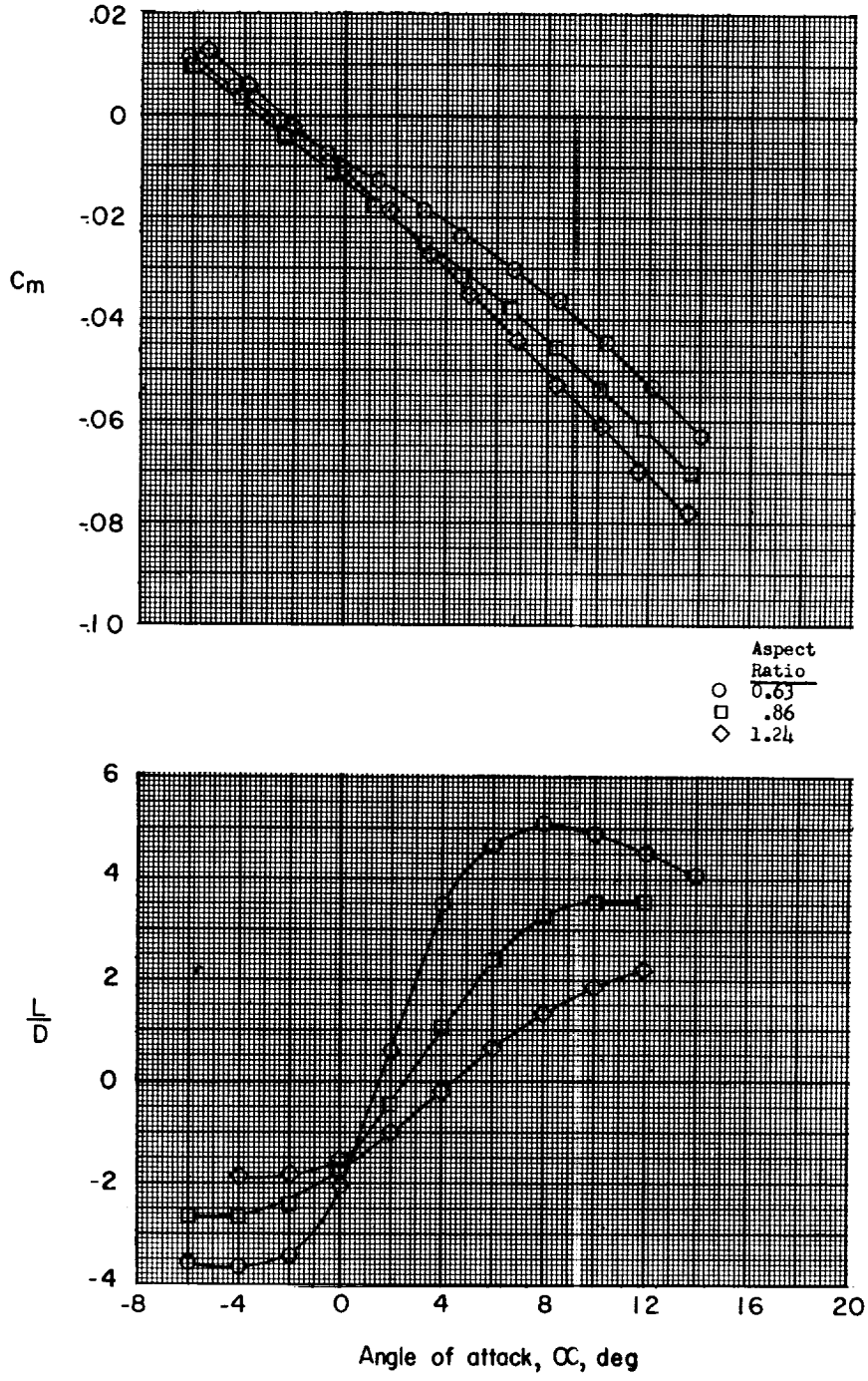

(b) Pitching-moment and L/D characteristics.

Figure 5.- Concluded.

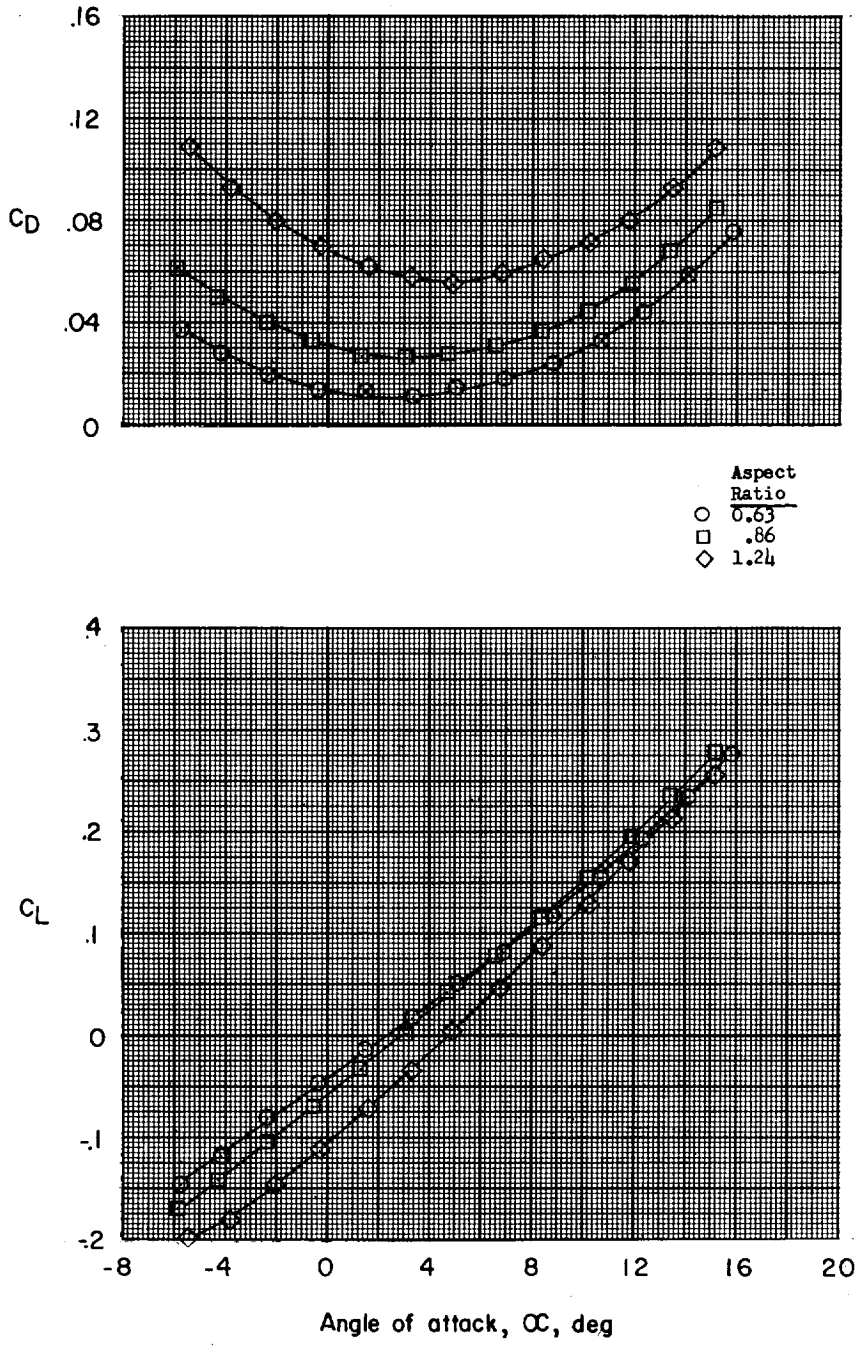

(a) Lift and drag characteristics.

Figure 6.- Longitudinal characteristics of wing models. Vertical tail on.

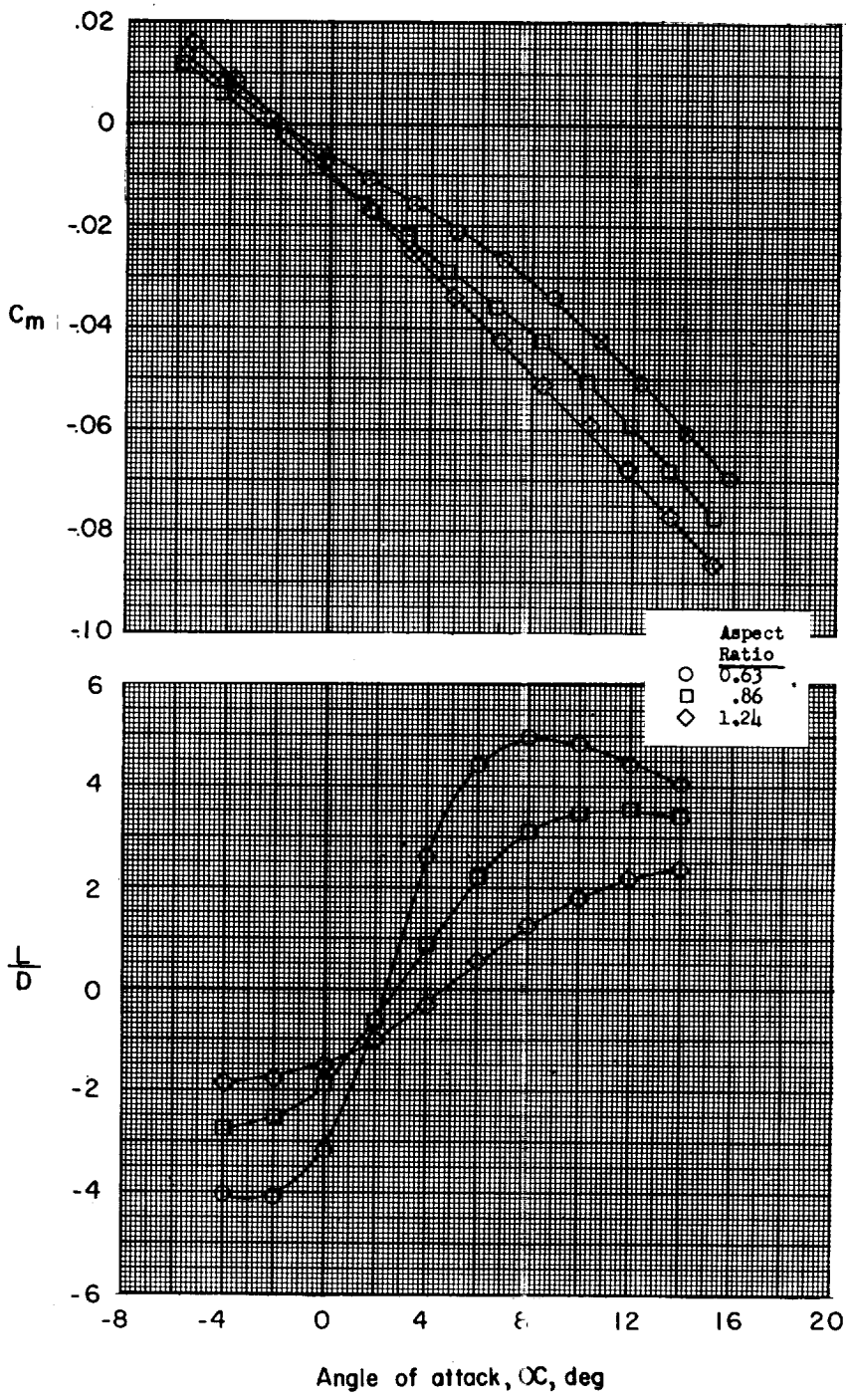

(b) Pitching-moment and L/D characteristics.

Figure 6.- Concluded.

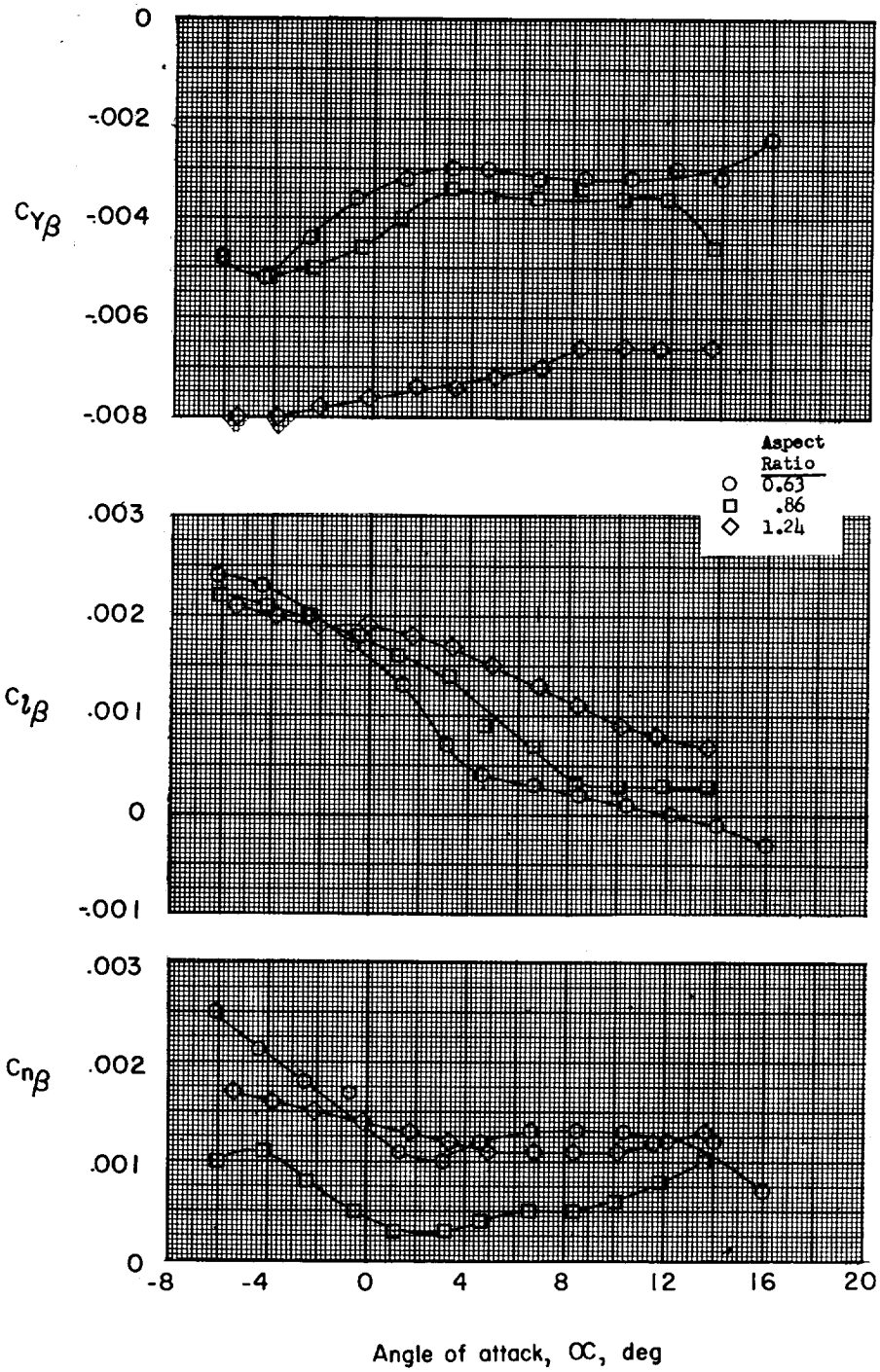

(a) Vertical tail off.

Figure 7.- Lateral-stability parameters of wing models.

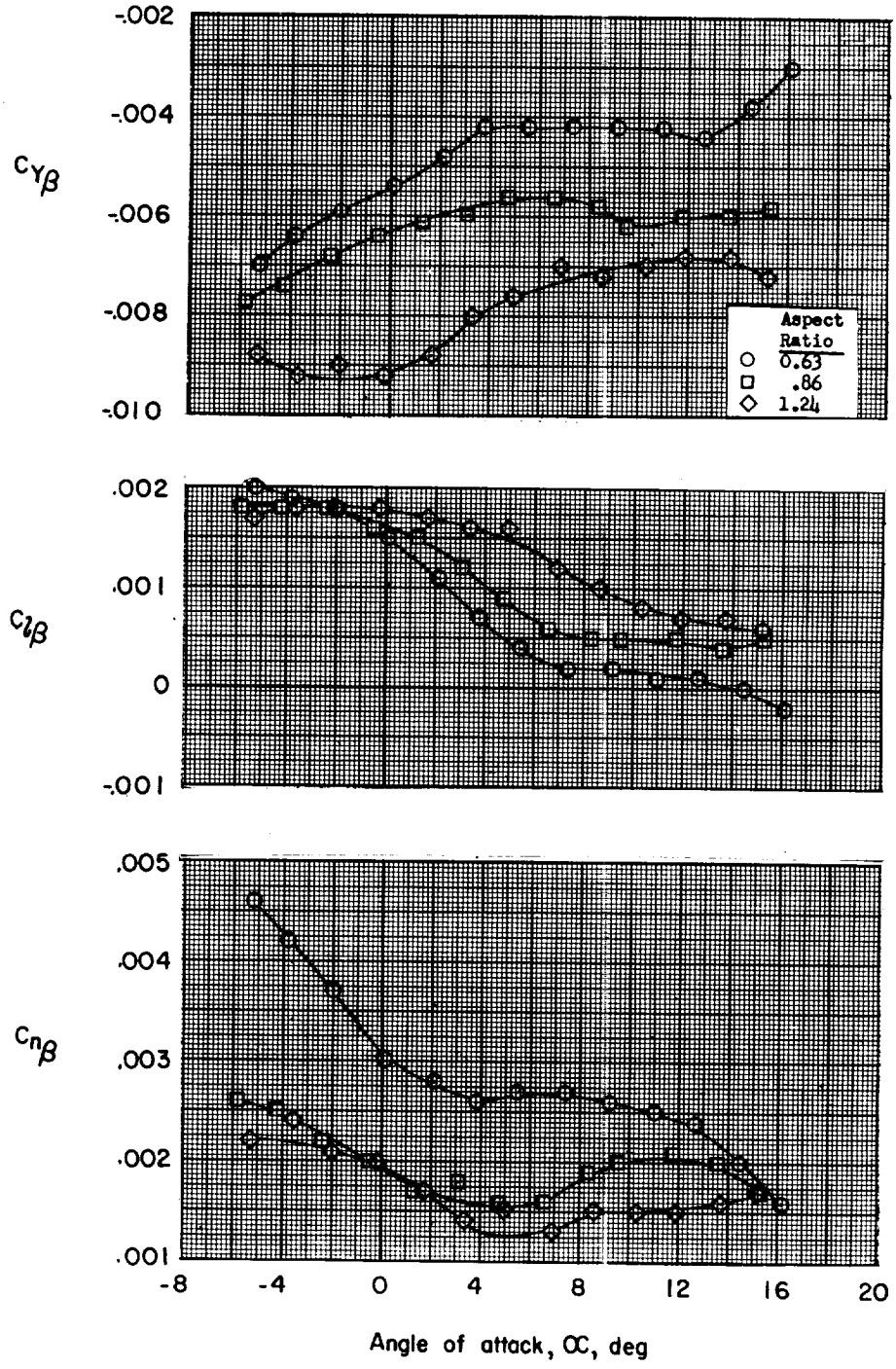

(b) Vertical tail on.

Figure 7.- Concluded.

NASA - Langley Field, Va. L-597